Analysis of water resources variability in the Yellow River of China using a distributed hydrological model

DAWEN YANG & WEIWEI SHAO

State Key Laboratory of Hydro-Science and Engineering, Department of Hydraulic Engineering, Tsinghua University, Beijing 100084, China

yangdw@tsinghua.edu.cn

Abstract Drying up of the main river along the lower reach of the Yellow River has occurred since 1972, and the situation has become more and more serious over the last 30 years. By incorporating historical meteorological data and the available geographic information related to the land surface conditions, a distributed hydrological model (GBHM) has been employed to simulate the natural runoff of this basin. Based on the simulated and observed river discharges, a quantitative analysis of the water resources in this basin over a long-term period of 50 years was carried out, which focuses on understanding the variability in the water resources due to climate change and human activity. In contrast to what might be believed based on common sense, it is found that the main reason for the aggravation of the drying up of the main river along the lower reach that occurred in the 1990s is climate change.

Key words Yellow River; water shortage; climate change; human activity; distributed hydrological model

INTRODUCTION

The scarcity of water resources is a major constraint for social and economic development in northern China and has led to widespread degradation of the natural ecosystem and environment. During the last 30 years the Yellow River has become a seasonal river. The drying up in the main river along the lower reaches started in 1972 and increased rapidly. In the most serious situation in 1997, the main river close to the sea dried up for more than 226 days, and the no-flow distance reached 704 km from the river mouth. Water shortages, especially the drying up of the main river along the lower reach in the Yellow River, have drawn a lot of attention from all over the world. Many studies have focused on finding the reason for this event. As a result of these studies, climate change and an increase in artificial water uses have been identified as the two main factors leading to the drying up of the river (Cheng *et al.*, 1999; Yang *et al.*, 2004). However, the details are not clear as to the effects of climate change and human activity over the long term.

On the other hand, historical climate data are generally available and provide a reference for studying the impact of climate change on water resources. However, due to the nonlinear behaviour of hydrological processes, changes in climate can not easily be converted into amounts of water resource change. Natural water resources need to be assessed by hydrological models using historical climate data as the input. Water balance models are commonly used for such purposes (Arnell, 1999). Middelkoop *et al.* (2001) compared a water balance model and a physically-based model for water resources assessment in the Rhine basin. It was found that a physically-based model did a better job than the water balance model in many cases. For the present study, an assessment of the natural river discharge was carried out by applying a distributed physically-based model for simulating the hydrological cycle over the last 50 years in the Yellow River basin. Based on the long-term hydrological simulation, the variability of water resources due to climate change and artificial uses are discussed.

METHODOLOGY

Data used in the study

The geographical information concerning the Yellow River basin used in this research is obtained from a number of global data sets. The digital elevation data of 1-km resolution is obtained from the USGS HYDRO1k data set. Land cover is obtained from the USGS Global Land Cover

Characteristics Data Base Version 2.0. This data has a spatial resolution of 1-km. For each vegetation type, a monthly leaf-area-index (LAI) is calculated from the monthly NDVI. A global data set of monthly NDVI with 8-km resolution is obtained from the DAAC of GSFC/NASA. This data set is available from 1982 onwards. The soil type is obtained from the Digital Soil Map of the World and Derived Soil Properties (FAO, 2003). It is developed at 5-minute resolution using the FAO-UNESCO soil classification. The soil properties used for the hydrological simulation include the porosity, the saturated hydraulic conductivity, and the other soil water parameters corresponding to each soil type in this map, are obtained from the Global Soil Data Task (IGBP-DIS, 2000). The water-retention relationship and unsaturated hydraulic conductivity are represented by Van Genuchten's formula, and the parameters are available in this data set.

The meteorological data from 1951 to 2000 were obtained from the China Administration of Meteorology, and is available at a daily temporal resolution at 108 gauges inside and close to the Yellow River basin (see Fig. 1). The discharge data collected before 1990 is from the "Hydrological Year Book" published by the Hydrological Bureau of the Ministry of Water Resources of China.

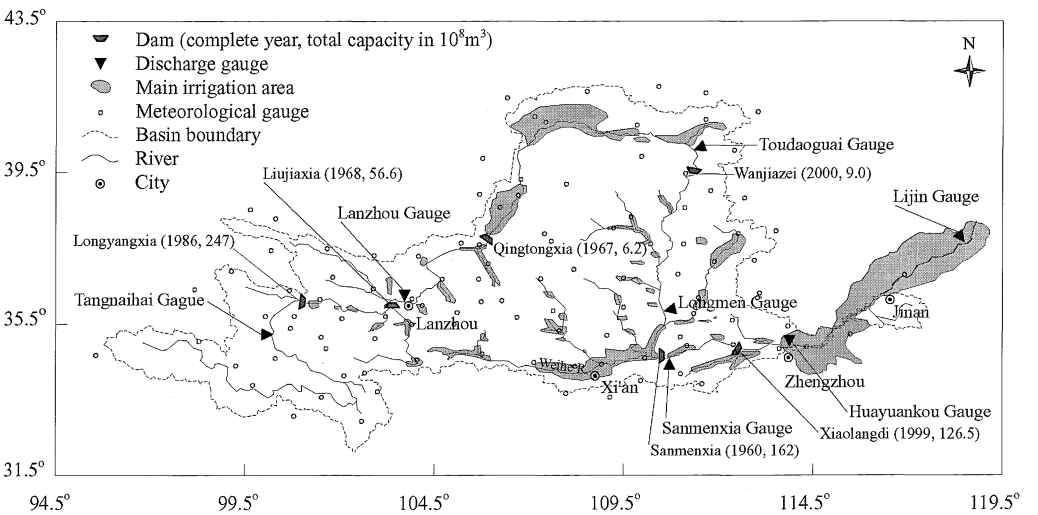

Fig. 1 The Yellow River basin.

Description of the distributed hydrological model-GBHM

The present study employs a distributed model for estimating the natural runoff in this basin over the last half century. The model uses a grid system with a 10-km spatial resolution, and runs in hourly time steps. Since there are significantly less drainage areas in the lower reach, most of the runoff is generated from the upstream of the Huayuankou gauge (see Fig. 1), and therefore the hydrological simulation only covers this area.

For subdividing the Yellow River basin, the Pfafstetter scheme (Yang *et al.*, 2003) is applied in the present study and a total of 137 sub-basins have been identified in the upstream of the Huayuankou gauge. The sub-grid parameterization used includes representations of the sub-grid variability in topography and land-cover. The topographical parameterization uses the catchment geomorphologic properties, which represent a grid by a number of hillslopes. The hillslopes located in a 10-km grid are grouped according to the land cover types. The hillslope is a fundamental computational unit for hydrological simulation. The geomorphology-based hydrological model (GBHM) (Yang *et al.*, 2002) is used for simulating the hillslope hydrology. The

hydrological processes included in this model are snowmelt, canopy interception, evapotranspiration, infiltration, surface flow, subsurface flow and the exchange between the groundwater and the river (Yang *et al.*, 2002). The actual evapotranspiration is calculated from the potential evaporation by considering seasonal variation of LAI, root distribution and soil moisture availability. This is computed individually from the canopy water storage, root zone and soil surface. Infiltration and water flow in the subsurface in the vertical direction and along the hillslope are described in a quasi-two-dimensional (2-D) subsurface model. The vertical water flow in the topsoil is represented by Richards equation and solved by an implicit numerical solution scheme. In this scheme, the topsoil is divided into a near surface layer of 5 cm, a root zone and a deep zone. The root zone and deep zone are again derived into sub-layers in the present model. The first layer is expected to be saturated during the rainfall period. Therefore, the upper boundary condition is given as constant soil water content for the rainfall cases. During the non-rainfall period, evaporation from the soil surface occurs, and the upper boundary condition is given as a constant flux. The soil water distribution along the hillslope is treated as uniform. The surface runoff is from the infiltration excess and saturation excess calculated by solving Richards equation. The surface runoff flows through the hillslope into the stream by a kinematic wave. The groundwater aquifer is treated as an individual storage corresponding to each grid. The exchange between the groundwater and the river water is considered as steady flow and is calculated by Darcy's law (Yang *et al.*, 2002). The runoff generated from the grid is the lateral inflow into the river at the same flow interval. Flow routing in the river network is solved using the kinematic wave approach.

Model calibration and validation

A 5-year test run from 1981 to 1985 was carried out to calibrate the model parameters. One of the calibrated parameters is the snowmelt factor in the temperature-based snowmelt equation. Another calibrated parameter, the hydraulic conductivity of the groundwater, is calibrated by checking the baseflow in different sub-basins. Model validation was carried out from 1986 to 1990 in the upstream of the Tangnaihai discharge station, where the human activity is insignificant, and the snowmelt runoff and groundwater flow are the main sources of river discharge. Figure 2 shows a comparison between the simulated and observed daily discharges at the Tangnaihai gauge for both the calibration and validation periods. Based on the daily discharges, the ratio of the absolute error to the mean and the Nash coefficient are calculated to be 19% and 0.88, respectively, for the calibration period and to be 17% and 0.89 for the validation period, respectively. A good agreement between the simulated daily hydrograph with the observed and a consistency of the simulations in both the calibration and validation periods are achieved.

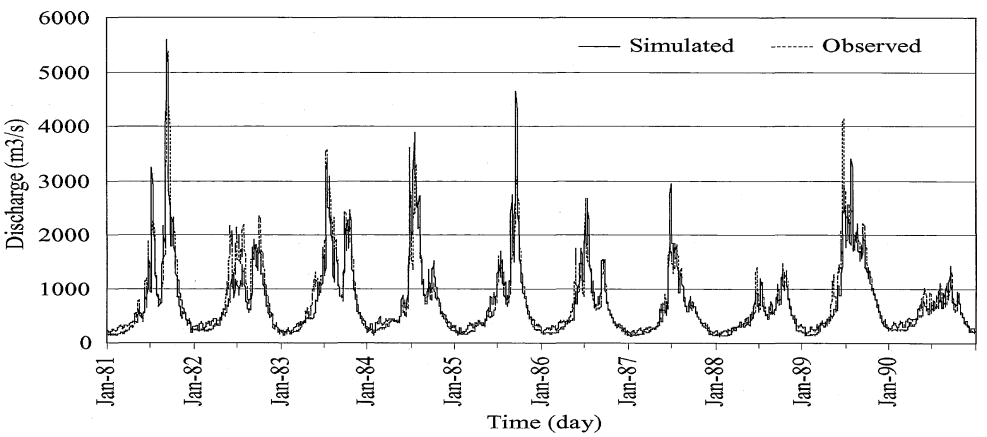

Fig. 2 Comparison of simulated and observed daily river discharge at Tangnaihai station.

ANALYSIS OF WATER RESOURCES IN THE LAST HALF CENTURY

Spatial and seasonal distribution of water resources for a long-term mean

By checking the 50-year average water balances covering the total study area, it was found that the annual precipitation, evaporation and runoff are 439 mm, 362 mm and 77 mm, respectively. The annual runoff consists of only 17.5% of the annual precipitation. High spatial variability of the hydrological characteristics can be seen in this basin. The annual precipitation ranges from 154 to 764 mm, which increases from north to south and from west to east. The annual actual evapotranspiration ranges from 137 to 589 mm (Fig. 3(a)). The Weihe basin and downstream of the Sanmenxia Dam have the highest evapotranspiration. The annual runoff ranges from 0 to 345 mm (Fig. 3(b)). The major source areas are located upstream of the Lanzhou gauge, the southern part of the Weihe River basin, and downstream of the Sanmenxia dam.

Considering the seasonal precipitation and water uses, the year may be divided into a dry season from November to June and a wet season from July to October. Table 1 shows the seasonal characteristics of the water resources in the study basin. The highly uneven distribution of the seasonal precipitation can be seen from Table 1, in which about 64% of the annual precipitation concentrates within the wet season from July to October. By the land surface hydrological processes, this seasonally-uneven distribution of precipitation is mediated in the river discharge in the upper regions but is amplified in the lower regions. For the whole of the simulated area, about 60% of the annual river discharge flows within the wet season from July to October.

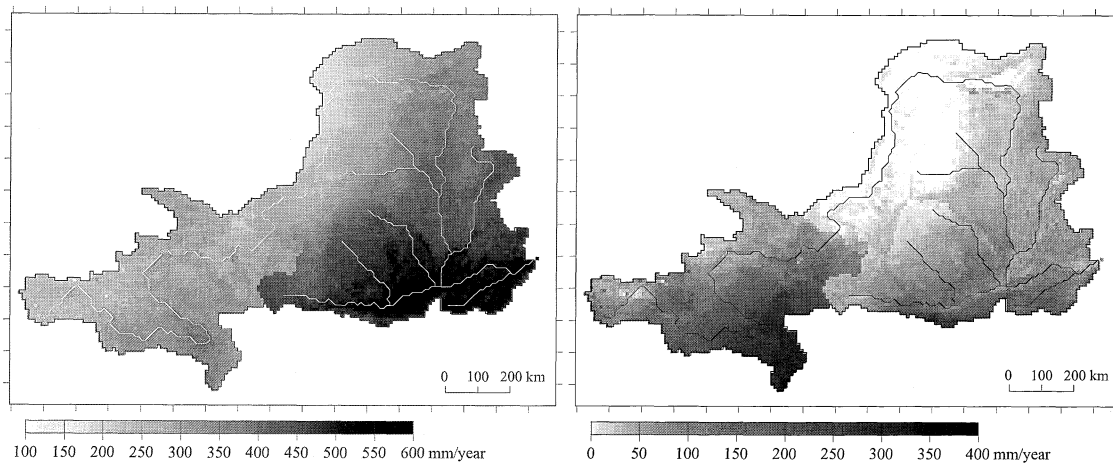

Fig. 3 Spatial distributions of 50-year means: (a) annual evapotranspiration, (b) annual runoff.

Table 1 Long-term average water balances from 1951 to 2000 for the dry season (November–June) and the rainy season (July–October).

Section *	Annual precipitation (mm)		Annual actual evaporation (mm)		Simulated annual river discharge (mm)	
	Dry	Rain	Dry	Rain	Dry	Rain
Upstream of Lanzhou	173	274	121	189	57	79
Lanzhou–Toudaoguai	83	180	113	139	6.6	5.6
Toudaoguai–Longmen	135	285	184	198	14.8	23.6
Longmen–Sanmenxia	204	344	238	230	27	53.7
Sanmenxia–Huayuankou	247	384	258	253	43.3	77
Whole study area	159	280	168	194	30	47

* The Yellow River basin is divided into six sections by the discharge gauges which correspond to the different characteristics of hydrology and water uses (see Fig. 1).

Reason for the drying-up of the main river along the lower reach over the last 30 years

Table 2 gives the historical records of river drying-up along the lower reaches over the last 30 years. A drying-up of the main river along the lower reach occurred from 1972, the situation continued during the 1980s and became worse in the 1990s. Figure 4 compares the annual available runoff and consumption with the no-flow duration along the lower reach in this basin over the last 30 years (1971–2000). It can be seen that the dry-ups occurred in the relatively dry years, especially during the whole of the 1990s, during which time the annual available runoff was less than the 30-year mean of 55 billion cubic meters. However, in contrast to common sense, the "drying-up" years do not correspond to the years of relatively high consumption of surface water. The annual variability in the consumption corresponds to the runoff availability. When less runoff is available, less surface water is consumed. The annual consumption of surface water shows a slightly decreasing trend is relation to the annual available runoff. It is concluded here that the aggravation of the drying-up situation in the 1990s is mainly caused by climate change. Table 3 summarizes the decadal averages of the water balance components for the whole simulation area. The variability of the natural runoff has a 10-year cycle. Comparing the basin averages in the two decades of the 1980s and the 1990s, the annual precipitation decreased by 38 mm and the annual mean temperature increased by 0.6°C. Consequently, the naturally available annual runoff decreased 24 billion cubic meters (36%) in the 1990s. In fact, the annual consumption of surface water in the 1990s decreased by 6.4 billion cubic meters (18%) compared to the 1980s. The ratio of the annual water consumption to the annual water available is 55% in the 1980s, but reaches 67% in the 1990s. As the result of both climate change and artificial consumption, annual runoff flowing into the sea decreases by nearly 43%. Keeping the similar trend of climate change, the Yellow River might cease to flow into the sea in future.

Table 2 Historical records of river drying up in the last 50 years.

Year	1971	1972	1973	1974	1975	1976	1977	1978	1979	1980
Days of no flow		19		20	13	8		5	21	8
Maximum distance of no flow (km)		310		316	278	166		104	278	104
Year	1981	1982	1983	1984	1985	1986	1987	1988	1989	1990
Days of no flow	36	10	5				17	5	24	
Maximum distance of no flow (km)	662	278	104				216	150	277	
Year	1991	1992	1993	1994	1995	1996	1997	1998	1999	2000
Days of no flow	16	83	60	74	122	136	226	142	42	
Maximum distance of no flow (km)	131	303	278	380	683	579	704	449	278	

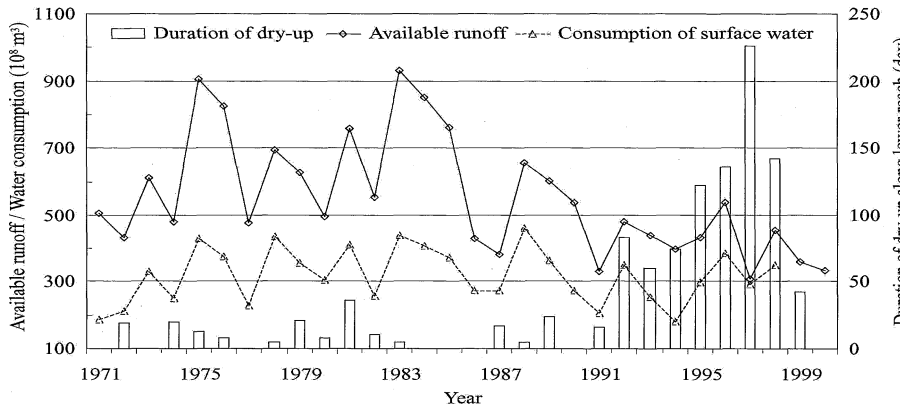

Fig. 4 Relationship between the annual available water and the duration of the drying-up.

Table 3 Decadal variations of water resources in the whole simulation area.

Component	1950s	1960s	1970s	1980s	1990s
Precipitation (mm/yr)	440.2	466.0	436.3	446.6	408.5
Annually mean temperature (°C)	6.22	6.38	6.61	6.69	7.31
Natural available water ($\times 10^8$ m^3/yr)	572.3	763.8	607.1	648.5	407.8
Artificial water consumption* ($\times 10^8$ m^3/yr)	134.0	236.4	312.4	355.1	273.4
Ratio of consumption to available (%)	23.4	30.9	51.5	54.8	67.1

* The difference between simulated and observed river flows.

For improving the no-flow condition along the lower reaches, two urgent countermeasures should be carried out: (1) protection of the water source areas, especially the upstream of the Lanzhou gauge, and (2) saving water usage along the middle and lower reaches. Protection of the upstream of the Lanzhou gauge should be emphasized here because the Chinese government is now promoting western development.

CONCLUSION

The spatial and seasonal distributions of water resources show high variability in the Yellow River basin. The major source area of the basin total annual runoff is located in the upstream of the Lanzhou gauge. About 60% of the annual precipitation is concentrated within the 4 months from July to October. The aggravation of the drying up situation in the 1990s is mainly a result of climate change because the 1990s were the driest period experienced in the last half century. A reduction in the water requirements from in the Yellow River basin is the only solution to the water shortage problem in the near future. The prediction of climate change and its effect on future water resources is also helpful for their management.

Acknowledgements This research was supported by the National Natural Science Foundation of China (no. 50721140161). The authors would like to express their appreciation for the grants received to aid in this research.

REFERENCES

Arnell, N. W. (1999) Climate change and global water resources. *Global Environ. Change* **9**, S31–S49.

Cheng, X., Li, X. & Lu, G. (1999) Characteristics of the river dry-up and variation of water resources in the Yellow River basin. *Adv. Sci. & Technol. of Water Resour.* **1**, 34–37 (in Chinese).

FAO (2003) Digital soil map of the world and derived soil properties. *Land and Water Digital Media Series Rev.* **1**.

IGBP-DIS (2000) Global Soil Data Products CD-ROM. International Geosphere-Biosphere Programme, Data and Information System, Potsdam, Germany. Available from Oak Ridge National Laboratory Distributed Active Archive Center, Oak Ridge, Tennessee, USA. http://www.daac.ornl.gov.

Middelkoop, H., Daamen, K., Gellens, D., Grabs, W., Kwadijk, J., Lang, H., Parmet, B., Schadler, B., Schulla, J. & Wilke, K.. (2001) Impact of climate change on hydrological regimes and water resources management in the Rhine basin. *Climate Change* **49**, 105–128.

Yang, D., Herath, S. & Musiake, K. (2002) Hillslope-based hydrological model using catchment area and width functions. *Hydrol. Sci. J.* **47**(1), 49–65.

Yang, D. & Musiake, K. (2003) A continental scale hydrological model using distributed approach and its application to Asia. *Hydrol. Processes* **17**, 2855–2869.

Yang, D., Li, C., Hu, H., Lei, Z., Yang, S., Kusuda, T., Koike, T. & Musiake, K. (2004) Analysis of water resources variability in the Yellow River basin during the last half century using the historical data. *Water Resour. Res.* **W06502**.